Improving frequency and ROCOF accuracy during faults, for P class Phasor Measurement Units

Andrew J. Roscoe, Graeme M. Burt
Department of Electronic and Electrical Engineering
University of Strathclyde
Glasgow, UK
Andrew.J.Roscoe@strath.ac.uk

Gert Rietveld
VSL Laboratory,
Delft, The Netherlands
G.Rietveld@vsl.nl

***Abstract*—Many aspects of Phasor Measurement Unit (PMU) performance are tested using the existing (and evolving) IEEE C37.118 standard. However, at present the reaction of PMUs to power network faults is not assessed under C37.118. Nevertheless, the behaviour of PMUs under such conditions may be important when the entire closed loop of power system measurement, control and response is considered. This paper presents ways in which P class PMU algorithms may be augmented with software which reduces peak frequency excursions during unbalanced faults by factors of typically between 2.5 and 6 with no additional effect on response time, delay or latency. Peak ROCOF excursions are also reduced. In addition, extra filtering which still allows P class response requirements to be met can further reduce excursions, in particular ROCOF. Further improvement of triggering by using midpoint taps of the P class filter, and adaptive filtering, allows peak excursions to be reduced by total factors of between 8 and 40 (or up to 180 for ROCOF), compared to the C37.118 reference device. Steady-state frequency and ROCOF errors during sustained faults or unbalanced operation, particularly under unbalanced conditions, can be reduced by factors of hundreds or thousands compared to the C37.118 reference device.**

Keywords—Power system measurements, Fourier transforms, Frequency measurement, Power system faults, Phase estimation, Power system state estimation, Power system parameter estimation

I. INTRODUCTION

The deployment and development of phasor measurement units (PMUs) and their applications continues apace. The current version of the standard IEEE C37.118 [1] describes the tests which a PMU should pass to be labelled "compliant". The standard also presents a Reference algorithm whose purpose is simply to demonstrate that the standard can be complied with, as a minimum level. However, the standard allows flexibility so that other algorithms can be used, which may have significantly better performance in some or all areas than the Reference algorithm. Development of the standard, and its relationship with the Reference algorithm, is on-going.

Proposed modifications to the standard include more relaxed specifications for frequency and ROCOF (rate of change of frequency, or RFE), since certain frequency and ROCOF results in [1] could not actually be achieved by the Reference algorithm. For some, the viewpoint is that the phasor measurement itself, i.e. amplitude and phase, is the key measurand and that frequency and ROCOF are not of such interest. Much of the recent academic literature concerning potential PMU algorithms (e.g. [2] [3] [4] [5]) places the focus firmly on the phasor measurement, with little or no treatment of frequency and/or ROCOF, while some consideration is given to frequency measurement in [6] and [7].

However, for some proposed PMU applications the measurements of frequency and ROCOF may be very important for control or protection actions. For example, frequency and ROCOF information is of key interest to control schemes such as load shedding [8] where thresholds in the range of 0.5 Hz and 0.2-1.5 Hz/s are of interest, with presumably a much finer measurement accuracy required. Users such as Hydro-Québec have also conducted detailed tests on the frequency measurements of PMUs [9], noting that post-fault frequency measurements with 12-50mHz error magnitudes are undesirable. This indicates that the robustness and accuracy of the frequency measurement is of high importance to their applications.

A set of candidate PMU algorithms has recently been presented [10],[11], based on a phase-by-phase Fourier analysis, using adaptive cascaded boxcar filters and frequency tracking, so that the filter centre frequency always falls as close as possible to the fundamental, that the filter zeros always fall as closely as possible to the unwanted harmonics, and that broadband interharmonic attenuation is as large as possible. The design of these algorithms was tailored to provide performance compliant to the C37.118 standard, and also to provide performance which significantly exceeded C37.118 requirements under the influences of off-nominal frequency, harmonics and interharmonics.

One aspect which is not addressed by the standard, and was not considered in [10],[11] or in much of the other recent literature on PMU algorithms, is the disturbances to PMU measurements during faults. However, utility customers are clearly are interested in how PMU reports may be disturbed by faults [9]. According to [9], the interest is particularly focused on the faster-reporting PMUs such as the P class device, and M class devices with reporting rates of F_S=50 or 60 Hz.

This is a postprint of a paper submitted to and presented at the IEEE International workshop on Applied Measurements for Power Systems (AMPS), 2013 [http://dx.doi.org/10.1109/AMPS.2013.6656233], and is subject to IEEE copyright.

In this paper the focus is on the P class device, under unbalanced faults. The deviations of frequency and ROCOF measurements are examined. Two fault scenarios are used to show how P class reports might be disturbed. The performance of the Reference algorithm from C37.118 is compared to that of modified algorithms, whose design is presented. These modified algorithms enable the undesired deviations of frequency and ROCOF to be reduced by significant factors, while still remaining compliant with C37.118 dynamic step and bandwidth tests.

II. P CLASS PMU ALGORITHMS

The Reference algorithm in C37.118 uses a core single-phase Fourier analysis section as shown in Fig. 1, using a fixed frequency for the quadrature oscillator and a fixed-weight triangular filter of length $(2/f_0)$ seconds, where f_0 is the nominal system frequency.

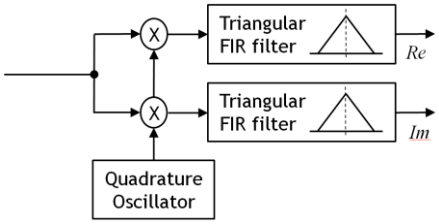

Fig. 1 Single-phase Fourier analysis section in the Reference algorithm

The adaptive algorithms referred to in this paper instead use a frequency-tracking algorithm to modify the quadrature oscillator frequency so that it tracks the system frequency f. The filter consists of cascaded boxcar filters, each of length $(1/f)$ seconds (Fig. 2). Details of this implementation are found in [10],[11]. The tracking is implemented by using parallel filter paths in an alternating fashion, described in [10],[11] as the "TickTock" algorithm. The filters are updated periodically so that at any time one of the filter paths is stable, symmetric (zero phase) and fully settled. This path can be used to obtain the results. In the meantime, the other path is reconfigured and the FIR filters are settling, until ready for use.

The cascaded boxcar filters together form a triangular filter, and if $f=f_0$, its performance is identical to the Reference algorithm.

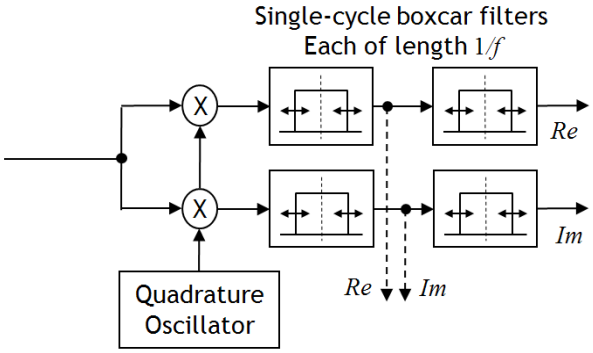

Fig. 2 Single-phase Fourier analysis section in the adaptive algorithms

The Reference algorithm from C37.118 (and also the algorithms in [10],[11]) combine the phasors from all three phases into a positive sequence phasor, before extracting the frequency and ROCOF information (Fig. 3).

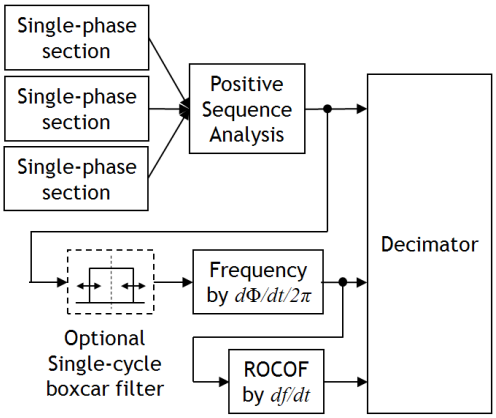

Fig. 3 Frequency calculation method, using positive sequence

In Fig. 3, the "optional single-cycle boxcar filter" was introduced in [11]. It was shown that for the P class devices, such a filter could be introduced to both the Reference and adaptive devices, with positive impacts for the stability of frequency and ROCOF outputs, and without violation of any C37.118 dynamic tests. This filter also provides benefits to the stability during faults, as will be shown later.

A. Weighted averaging of single-phase frequencies

The main contribution of this paper is to modify the frequency measurement section shown in Fig. 3, so that the frequency is determined from a weighted average of three frequencies measured from the individual phases. There are several advantages of doing this.

During unbalanced operation the measurement is more stable. The extreme case is if a three-phase PMU is used at a location where only a single-phase connection is available, all three inputs can be connected to the same phase. The positive sequence phasor will have zero magnitude, but the weighted-average method will allow frequency to be measured as normal. During less extreme unbalance, the frequency measurements can be weighted from each phase, so that signals with amplitudes of about 1.0pu have the highest weightings, but signals with lower or higher amplitudes have lower weightings, to represent the poorer signal-to-noise or distortion properties that are likely at off-nominal conditions.

When a fault occurs, the amplitude(s) on the faulted phase(s) change transiently, then may approach some stable unbalanced quantity if the fault persists, then may transiently revert to normal values when the fault is cleared. During the transient phases, the Fourier correlation results are imperfect. Impact on the measured phasor itself may only be small, but the impact on frequency and ROCOF, through the differentiation actions, can be excessive. By suitably adjusting the weighting functions to favour the phases which appear to be least perturbed during transients, it is likely that much of the unwanted frequency and ROCOF deviations can be avoided.

Fig. 4 shows how such a weighted averaging can be carried out, as a replacement algorithm to that of Fig. 3.

This is a postprint of a paper submitted to and presented at the IEEE International workshop on Applied Measurements for Power Systems (AMPS), 2013 [http://dx.doi.org/10.1109/AMPS.2013.6656233], and is subject to IEEE copyright.

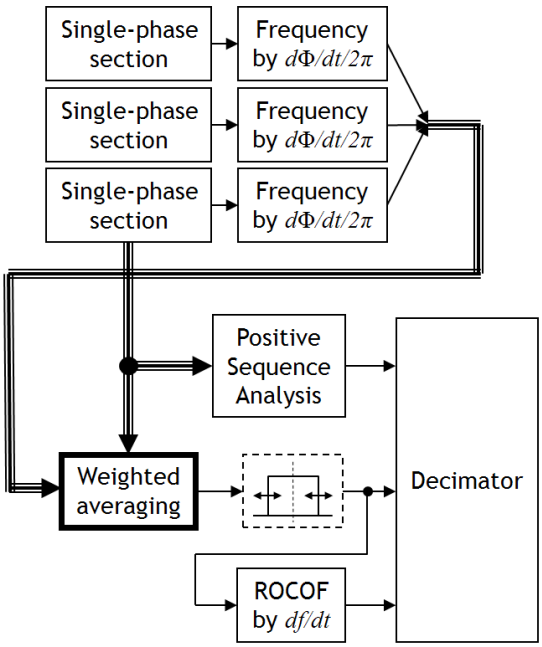

Fig. 4 Frequency calculation method, using weighted averaging

The challenge is to create the weights w for the averaging process. The algorithm of Fig. 5 has been used in this paper.

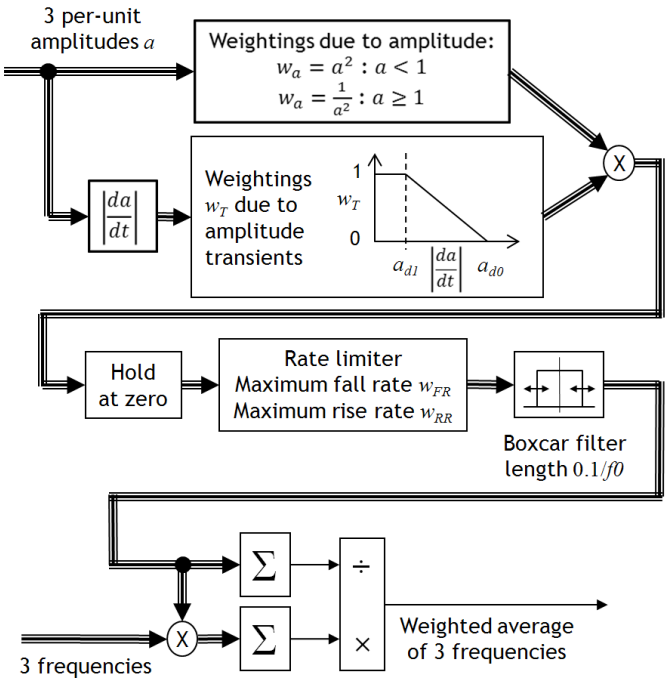

Fig. 5 Calculating the weights for the averaging, and the weighted averaging process

For P class, in Fig. 5, the following values are generally suitable: a_{d1}=0.03f_0, a_{d0}=0.1f_0, w_{FR}=(f_0/0.2), w_{RR}=(f_0/3). In particular the parameter a_{d1} needs to be large enough to avoid spurious triggering during C37.118 bandwidth testing, or during normal applications of interharmonics. These effects were examined in [11] and a *da/dt* triggering value of 0.03pu/cycle was found to be supportable.

The weightings are passed through a rate limiter which limits their maximum fall-rate and rise-rate. This is an important stage because if the weight for a particular phase is suddenly changed, this can result in a sudden change in frequency output from the weighted averaging block at the bottom of Fig. 5, leading to a misleading ROCOF output. On the other hand, if the falling ramp-rate is too slow, the weighting(s) of the faulted phase(s) cannot reach zero quickly enough and the weighted averaging algorithm will be ineffective at ignoring the data from the faulted phase(s). The falling ramp-rate is therefore set quite aggressively at $5f_0$ s^{-1}, so that the weight can drop from 1 to 0 in 1/5th of a cycle. The rising ramp-rate limit can be much slower at f_0/3 s^{-1}, allowing a rise from 0 to 1 over 3 cycles. During post-fault conditions, the weighting recovers only slowly as oscillations die away. The "Hold at Zero" is a function which latches the weight(s) at zero for a time of ($2/f_0$) seconds if it reaches zero, before the weight(s) are allowed to begin rising again. This minimises unwanted disturbances during partial-depth single and phase-phase faults where the weights can initially drop to zero due to the detection of initial amplitude transients (via *da/dt*) but could otherwise recover during the fault to non-zero values even though the faulted phases are distorted and can lead to unwanted perceptions of frequency and ROCOF deviations.

When a transient is detected, the output of the rate limit filter tends to be a linear slope from a weighting of near-unity to zero. This gradual ramping is required in order to avoid discontinuities in the averaged value of frequency (and hence spikes in ROCOF), which could result if a weighting is suddenly reduced from 1 to 0, for example. In fact, it was found that even the distinct starts and end of the ramped weights caused spikes in the measured ROCOF outputs. Therefore, the small additional boxcar filter with length 0.1 cycle in Fig. 5 is added. It modifies the weight trajectory to more of an "S" curve; in particular the start and end of the ramp which are smoothed. This helps to further reduce spurious ROCOF measurements.

B. *1-cycle triggering from the "mid tap"*

The key to reducing measurement excursions is reducing the time taken to initiate triggering, while retaining a smooth ramp of weights so that the frequency output is continuous. The adaptive algorithms offer an additional feature here in that data from the "mid tap" of the filter is available, with a 1-cycle latency (Fig. 2). This allows a faster triggering. The drawback is that the measured *da/dt* from this 1-cycle measurement is subject to higher levels of interference from interharmonics and coupled effects on un-faulted phases. In this paper, for the faster 1-cycle triggered methods, the following parameters are therefore adjusted: a_{d1}=0.1f_0, a_{d0}=0.3f_0, w_{FR}=(f_0/0.1).

III. Simulations and Results

To show the benefit of the weighted averaging techniques, a simple 3-phase simulation of a faulted line is carried out in MATLAB® Simulink using the "Distributed Line" models in SimPowerSystems. This simulation (Fig. 6) uses the same scenarios as given in [12], [13].

This is a postprint of a paper submitted to and presented at the IEEE International workshop on Applied Measurements for Power Systems (AMPS), 2013 [http://dx.doi.org/10.1109/AMPS.2013.6656233], and is subject to IEEE copyright.

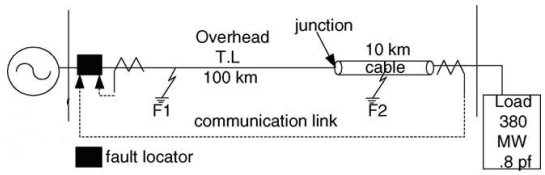

Fig. 6 110kV combined line-cable connection

A single-phase to ground fault is applied 44.54km from the sending end, and a phase-phase (B-C) fault is applied 20km from the sending end. The frequency and ROCOF errors are assessed from P class PMU algorithms, using the voltages at the receiving end of the line. The applied frequency at the sending end is 48Hz, deliberately off-nominal to further stress the algorithms. The following 4 algorithms are compared:

1) Reference algorithm (Fig. 1 and Fig. 3).
2) Reference algorithm with weighted averaging (Fig. 1 and Fig. 4
3) Adaptive algorithm with weighted averaging (Fig. 2 and Fig. 4) using the 2-cycle trigger.
4) Adaptive algorithm with weighted averaging (Fig. 2 and Fig. 4) using the 1-cycle trigger from the "mid tap".

Also, all four algorithm variants are tested in two conditions, firstly without the optional single-cycle boxcar frequency filter (Fig. 3 and Fig. 4), and then with this extra filtering added.

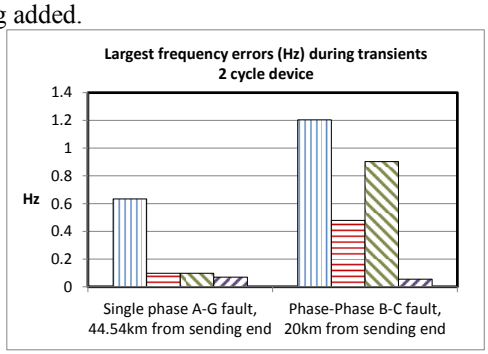

(a)

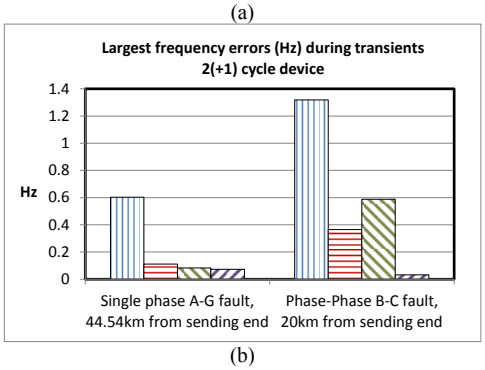

(b)

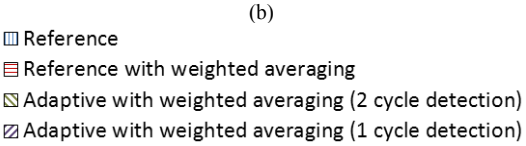

Fig. 7 Largest frequency errors during fault inception, presence and clearance.
(a) without optional single-cycle frequency filtering,
(b) with optional single-cycle filtering.

Fig. 7 shows the peak unwanted frequency excursions during the faults (covering fault inception, duration and clearance), extracted from the PMU algorithms at their full 10kHz sample rate, therefore representing the worst case values which might appear in reports when downsampled to F_S=50 Hz. The positive impact of the weighted averaging algorithms is clear to see, in particular the significant reductions enabled when the 1-cycle triggering method is applied. The worst case error can be reduced from 0.6-1.2 Hz to <0.1 Hz.

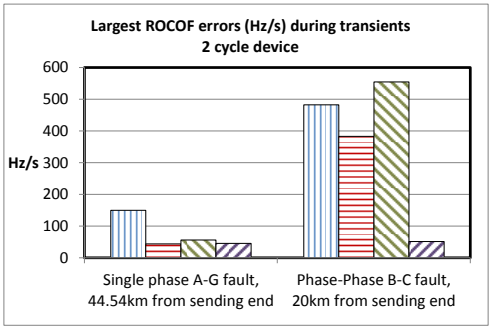

(a)

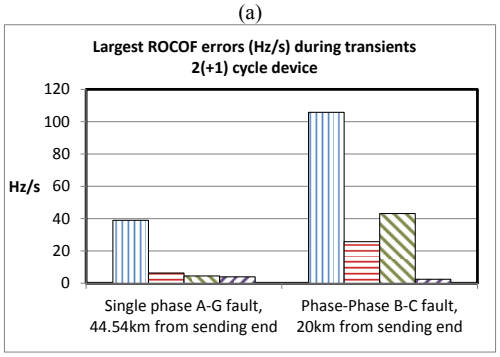

(b)

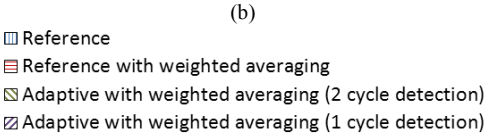

Fig. 8 Largest ROCOF errors during fault inception, presence and clearance.
(a) without optional single-cycle frequency filtering
(b) with optional single-cycle filtering.

The peak ROCOF errors are shown in Fig. 8. Again, the benefit of the proposed weighted averaging schemes is clear. Note the different scales on Fig. 8. a) and b). For ROCOF, the addition of the optional 1-cycle frequency filter also leads to a significant reduction in error. Overall, peak ROCOF error can be reduced from 150-500 Hz/s to 2.6-4 Hz/s.

A. Time domain response

To demonstrate operation of the algorithm, the following data shows how the algorithm performs in the time domain. The example used is the phase-phase (B-C) fault, measured by the adaptive PMU using 1 cycle detection, and the optional single-cycle filtering. This scenario corresponds to the far-right bar on Fig. 7b and Fig. 8b.

This is a postprint of a paper submitted to and presented at the IEEE International workshop on Applied Measurements for Power Systems (AMPS), 2013 [http://dx.doi.org/10.1109/AMPS.2013.6656233], and is subject to IEEE copyright.

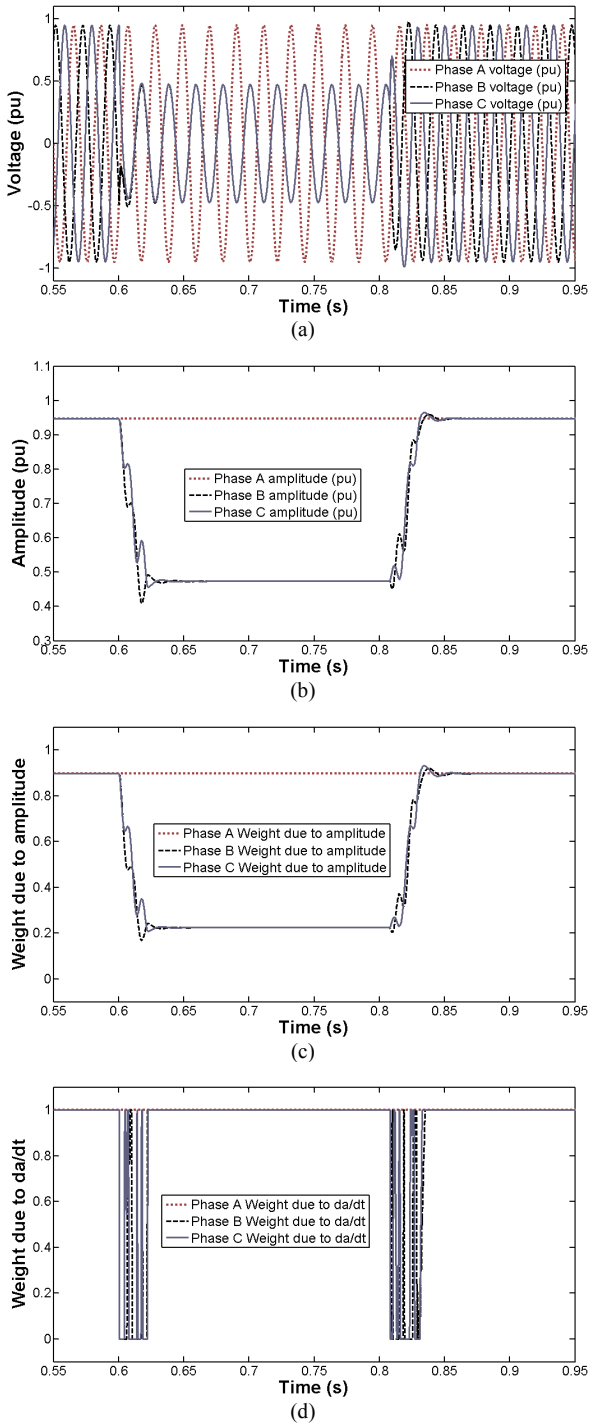

Fig. 9 Time domain example.
(a) voltages on each phase
(b) measured voltage amplitudes (1 cycle measurement)
(c) weights due to amplitude
(d) weights due to *da/dt*

The traces of sampled voltage, measured amplitude (over 1 cycle), weightings, frequencies (of each phase), and weighted average frequency, are shown on Fig. 9 and Fig. 10. The voltages on phases B and C (relative to ground) overlay during the fault as they are shorted together (Fig. 9a & b). There are also aperiodic components present during the fault inception and clearance periods, and the measured amplitudes do not change in a linear fashion, containing reversals in gradients *da/dt*. Measured phase angles (not shown) also transition likewise and this is one reason that measuring frequency and ROCOF directly from the positive sequence vector is susceptible to large errors during such faults.

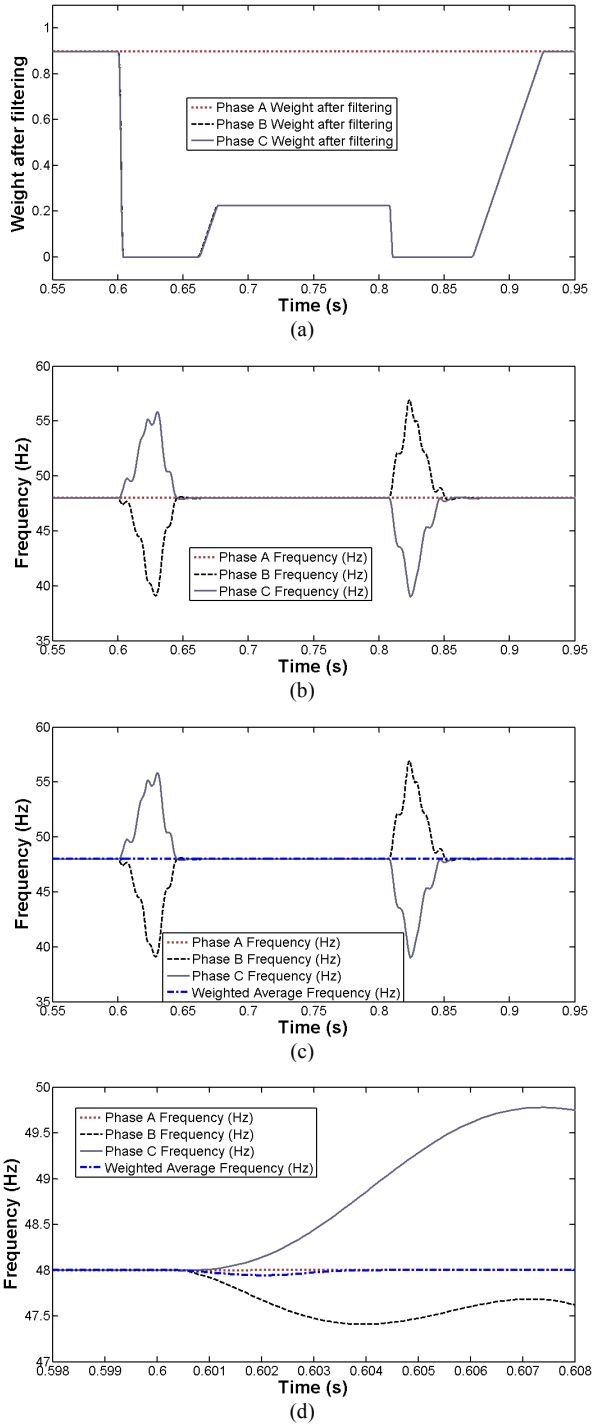

Fig. 10 Time domain example.
(a) weights after filtering
(b) frequencies measured on each phase
(c) weighted average frequency overlaid
(d) close-up of fault inception during first 8ms post-fault

This is a postprint of a paper submitted to and presented at the IEEE International workshop on Applied Measurements for Power Systems (AMPS), 2013 [http://dx.doi.org/10.1109/AMPS.2013.6656233], and is subject to IEEE copyright.

The measured amplitudes (over 1 cycle) for phases B and C drop to ~0.47pu during fault inception (Fig. 9b). The weightings due to amplitude drop to ~0.22 (Fig. 9c), by the process of Fig. 5. The transient weightings for phases B and C oscillated rapidly between 0 and 1 during fault inception, as the gradient *da/dt* changes and reverses (Fig. 9d). The combination of both types of weighting, followed by the filtering, leads to the weightings shown in Fig. 10a. The information from phase B and C is disregarded entirely during much of the fault inception and clearance, and has a low but non-zero weighting during the sustained fault when the phase B and C waveforms are relatively stable but have lower amplitudes than phase A. The phase A weighting remains stable it its original value, close to unity.

Fig. 10b shows the frequency which is determined from each of the 3 phases. The frequency measured on phase A is hardly disturbed, while that of phases B and C is significantly disturbed. In this case the frequency deviation measured on phases B and C tends to be opposite, due to the phase shifts of Fig. 9a, but they are not exactly opposite due to resonance and settling effects. For this reason, ignoring them as far as possible is desirable. Fig. 10c shows how the weighted average of frequency almost exactly overlays the phase A data. To show more detail, Fig. 10d highlights the averaging process during the first 8ms following fault inception. Clearly an unweighted average would have produced a much greater frequency deviation than the weighted average process returns.

IV. CONCLUSIONS

The implementation of a weighted average calculation of frequency (and also ROCOF) has been shown to be able to provide significant reductions in the unwanted excursions of frequency and ROCOF measurements from P class PMUs during faults. The techniques could also be applied to M class devices with appropriate modification to the triggering and rate limiting detectors/filters. The maximum possible reduction in peak frequency excursions for P class devices, relative to the C37.118 Reference algorithm, is a factor between 8 and 40 for the 2 fault simulation cases shown. For ROCOF, the factors are between 36 and 180. The factors can be even higher when only the periods between fault inception and clearance are considered (steady-state fault conditions), when the voltages can be highly unbalanced and frequency can be off-nominal. In these situations, the frequency-tracking nature of the adaptive algorithms plays a significant part of the reduction.

Since this PMU can detect faults, the PMU could generate a "fault detected" signal embedded within the PMU report. This could be used to initiate a new state estimation as described [14], saving higher-level algorithms from trying to determine the presence of faults from abnormal PMU report values.

Only amplitude and rate-of-change-of-amplitude (*da/dt)* was considered to determine the weights and fault detection. However, $d\Phi/dt$ might also be considered, with additional benefits. Inplementing $d\Phi/dt$ can be non-trivial due to phase-wrapping issues. However, background work has already been done in [11] which gives guidelines to acceptable trigger levels, and presents a suitable algorithm for detecting $d\Phi/dt$.

An entirely alternative approach to determining the weightings might be to calculate ROCOF independently for each of the 3 phases within the PMU, on an un-weighted basis. The weightings could be calculated via a function which favours the phases showing the smallest values of ROCOF. This might result in a simpler weight-determination algorithm with less reliance on rate-limiting filters and "hold" operations. Such a scheme has not yet been investigated.

The use and application of any the above techniques could also be explored and extended for use within M class devices.

REFERENCES

[1] IEEE, "IEEE Standard for Synchrophasor Measurements for Power Systems," C37.118.1-2011, 2011.

[2] D. Belega and D. Petri, "Accuracy Analysis of the Multicycle Synchrophasor Estimator Provided by the Interpolated DFT Algorithm," *IEEE Transactions on Instrumentation and Measurement,* vol. 62, pp. 942-953, May 2013.

[3] P. Castello, M. Lixia, C. Muscas, and P. A. Pegoraro, "Adaptive Taylor-Fourier synchrophasor estimation for fast response to changing conditions," *2012 IEEE International Instrumentation and Measurement Technology Conference (I2mtc),* pp. 294-299, 2012.

[4] P. Castello, M. Lixia, C. Muscas, and P. A. Pegoraro, "Impact of the Model on the Accuracy of Synchrophasor Measurement," *IEEE Transactions on Instrumentation and Measurement,* vol. 61, pp. 2179-2188, Aug 2012.

[5] G. Barchi, D. Macii, and D. Petri, "Effect of Transient Conditions on DFT-based Synchrophasor Estimator Performance," in *IEEE AMPS 2012 Applied Measurements for Power Systems*, Aachen, Germany, 2012.

[6] J. A. D. Serna and J. Rodriguez-Maldonado, "Taylor-Kalman-Fourier Filters for Instantaneous Oscillating Phasor and Harmonic Estimates," *IEEE Transactions on Instrumentation and Measurement,* vol. 61, pp. 941-951, Apr 2012.

[7] J. A. D. Serna, "Synchrophasor Estimation using Prony's Method," *IEEE Transactions on Instrumentation and Measurement,* (In Press).

[8] J. Tang, J. Liu, F. Ponci, and A. Monti, "Adaptive Load Shedding Based on Combined Frequency and Voltage Stability Assessment Using Synchrophasor Measurements," *IEEE Transactions on Power Systems,* vol. 28, pp. 2035-2047, 2013.

[9] I. Kamwa, S. R. Samantaray, and G. Joos, "Compliance Analysis of PMU Algorithms and Devices for Wide-Area Stabilizing Control of Large Power Systems," *IEEE Transactions on Power Systems,* vol. 28, pp. 1766-1778, 2013.

[10] A. J. Roscoe, I. F. Abdulhadi, and G. M. Burt, "P and M Class Phasor Measurement Unit Algorithms using Adaptive Cascaded Filters," *IEEE Transactions on Power Delivery,* vol. 28, pp. 1447-1459, 2013.

[11] A. J. Roscoe, "Exploring the relative performance of frequency-tracking and fixed-filter Phasor Measurement Unit algorithms under C37.118 test procedures, the effects of interharmonics, and initial attempts at merging P class response with M class filtering," *IEEE Transactions on Instrumentation and Measurement,* vol. 62, pp. 2140-2153, 2013.

[12] M. Popov, G. Rietveld, V. Terzija, and Z. Radojevic, "An Efficient Algorithm for Fault Location on Mixed Line-Cable Transmission Corridors," in *International Conference on Power Systems Transients (IPST)*, Vancouver, Canada, 2013.

[13] E. S. T. El Din, M. M. A. Aziz, D. K. Ibrahim, and M. Gilany, "Fault location scheme for combined overhead line with underground power cable," *Electric Power Systems Research,* vol. 76, pp. 928-935, Jul 2006.

[14] P. M. Ashton, G. A. Taylor, M. R. Irving, I. Pisica, A. M. Carter, and M. E. Bradley, "Novel Application of Detrended Fluctuation Analysis for State Estimation Using Synchrophasor Measurements," *IEEE Transactions on Power Systems,* vol. 28, pp. 1930-1938, 2013.

This is a postprint of a paper submitted to and presented at the IEEE International workshop on Applied Measurements for Power Systems (AMPS), 2013 [http://dx.doi.org/10.1109/AMPS.2013.6656233], and is subject to IEEE copyright.